Available online at www.sciencedirect.com
ScienceDirect
International Journal of Pressure Vessels and Piping 84 (2007) 739–748
INTERNATIONAL JOURNAL OF Pressure Vessels and Piping
www.elsevier.com/locate/ijpvp

Experimental determination of stress corrosion crack rates and service lives in a buried ERW pipeline

Pablo Gabriel Fazzini, Jose Luis Otegui*

University of Mar del Plata, Juan B. Justo 4302, 7600 Mar del Plata, Argentina

Received 24 February 2006; received in revised form 24 May 2007; accepted 30 May 2007

Abstract

Threshold stresses and crack growth rates for in-service stress corrosion cracking (SCC) of two electrical resistance weld (ERW) seam welded pipes from two 45-year-old oil pipelines were experimentally assessed. Seventeen high-pH SCC tests were carried out, in both base and ERW weld metals, at two temperatures (73 and 45 °C). Tapered specimens were used for base metal, and constant section specimens were developed for ERW tests, in which original surface conditions were preserved. It was found that susceptibility of the ERW seam welds is much higher than for base materials, so that the welds define the length of the pipe that is susceptible to SCC. Threshold pressure estimates for SCC initiation were defined from tests at elevated temperature, service temperature, and literature correlations. Fabrication residual stresses were also measured and taken into consideration. SCC threshold pressures for these lines are controlled by the ERW welds; the pipe tracts that are considered to be susceptible to SCC are those that undergo a service pressure of at least 2.4 MPa. For the case under study, this represents about 70% of the length of the pipeline.

Keywords: SCC test; Crack growth rate; Threshold stress; ERW; Pipeline integrity

1. Introduction

A number of causes have been found to produce in-service degradation in buried oil and gas transmission pipelines, related to mechanical and environmental damage. Typical environmental in-service damage types are: corrosion, hydrogen stress cracking and stress corrosion cracking. Stress corrosion cracking (SCC) is a term used to describe service failures in engineering materials that occur by slow environmentally induced crack propagation. This phenomenon is associated with a combination of stress (applied or residual) above some threshold value, specific environment and in some systems metallurgical conditions, which lead to surface cracks with a high aspect ratio (long and shallow). SCC has been recognized as a cause of failures in high-pressure gas and oil transmission lines since the mid-1960s [1–3]. SCC on the outer surface of pipelines has occurred in several countries throughout the world (Australia, Iran, USA, Canada, the former Soviet Union and Pakistan) and contributes to major failures in pipelines.

Two forms of SCC in the outer surface of buried pipelines have been identified: high-pH or "classical SCC" and low pH or "near neutral SCC". Both types of SCC have only been observed under disbonding coatings and it is generally accepted that a fluctuating stress component is required for crack growth. Low-pH or near-neutral SCC on the outer surface of pipelines is associated with specific soil conditions at free corrosion potential, where cathodic protection is ineffective. In this type of SCC there is no correlation with temperature; crack morphology is transgranular and evidence of substantial side-wall corrosion is normally found. Low-pH SCC occurs in the presence of dilute solutions of carbonate–bicarbonate having a pH of around 6 (good tap water with a little bit of CO_2).

The high-pH form is by far the most reported form of SCC. High-pH SCC on pipelines is characterized by the presence of patches or colonies of numerous fine, usually very shallow, longitudinal intergranular cracks with little evidence of secondary corrosion [4]. Cracking is associated

*Corresponding author. Tel.: +54 223 481 6600; fax: +54 223 481 0046.
E-mail addresses: pgf@fi.mdp.edu.ar (P.G. Fazzini), jotegui@fi.mdp.edu.ar (J.L. Otegui).

0308-0161/$ - see front matter © 2007 Published by Elsevier Ltd.
doi:10.1016/j.ijpvp.2007.05.008

with relatively concentrated carbonate–bicarbonate solutions [5] having pH values of approximately 9. The growth rate of this type of SCC depends exponentially on temperature and stress level [6]. Because of this, the number of failures falls markedly with increased distance from compressor and pump stations. Cathodic protection (CP) plays an important role in high-pH SCC because the range of electrochemical potentials for highest susceptibility is between −600 and −750 mV ($Cu/CuSO_4$), and CP is effective in achieving these potentials under disbonded coatings.

The Argentine high-pressure oil and gas transmission pipeline system includes more than 40,000 km of buried piping. Surface coatings are mostly of the tar and glass fibre type. Longitudinal tube seams are made with both electrical resistance welding (ERW) and double submerged arc welding (DSAW). Diameters range from less than 14 to 36 inches (350–900 mm). Construction dates of most of these pipes range from around 1960 to around 1980. Until 10 years ago, there had been no record of SCC damage identified as the main cause of failures in Argentine pipelines. As most of the pipeline systems have reached a certain age, this mechanism is now apparently starting to have an important impact on pipe reliability.

In a previous study by the authors [7], the causes of three blowouts that occurred in different oil and natural gas transmission pipelines in Argentina were analyzed. In this paper, further experimental SCC studies in base metal and seam weld metal of an ERW 350 mm (14″) diameter oil pipeline are presented. The maximum operating temperature is 45 °C, immediately downstream from the pumping stations.

Longitudinal welds generate stress raisers, residual stresses and metallurgical changes. Transverse residual stresses are about half the yield strength of the base material. The ERW seam-welded pipes are made by rolling a plate between clamps, pushing both edges until electric contact is made, and then heating under loading to melt and produce the weld. These processes generate perimeter displacements that produce elastic circumferential stresses in the material. After cooling of the weld bead, a circumferential residual stress distribution is left, which is tensile in the outer surface, where the SCC cracks are later initiated.

Defects typically associated with ERW, especially to those welds carried out at low frequency, are due to incomplete joining and internal defects (inclusions, lack of fusion, etc.) in the middle area of the weld [8]. One typical form of defect is the so-called hook crack, in which an inclined crack is formed a couple of millimeters away from the weld center line, following the lamination planes [9]. During the weld process, the heated material is ejected from the center of the thickness toward the surfaces of the pipe. Lamination defects, originally parallel to the surface, are reoriented through the thickness. This decreases the resistance of the weld to circumferential stresses. The ejected material is eliminated mechanically with a cutting tool, in a process called shaving. This process leaves marks on the surfaces that work as possible crack initiation areas. Subsurface plastic deformation due to shaving also creates a very local state of residual tensile stresses in the through-thickness direction. Both surface marks and subsurface residual stresses could greatly influence the conditions for SCC crack initiation.

Given the particular metallurgical, mechanical and geometrical conditions of the welds, and their possible influence on the susceptibility to SCC, both base metal and longitudinal welds of the pipes were assessed. Well-known methods for evaluating the susceptibility to SCC are focused only in base material [10], and require relatively large test specimens. The small width of the weld precludes the use of such specimens, so that a new test specimen was designed.

2. Experimental procedure

Mechanical properties of the materials under investigation are shown in Table 1. The tube material complies with the requirements of the API 5 L X 46 standards [11]. Hardness and microhardness Vickers tests of base and weld metals show low hardness in base material (20 HRC). In the central area of the longitudinal welds, an increase of hardness is reported up to 30 HRC, making the welds marginally susceptible to hydrogen embrittlement. This higher hardness coincides with a change in microstructural characteristics, which is ferritic pearlitic in base metal and lower bainitic or martensitic in the highly deformed area of the weld centerline. It also coincides with a higher strength and lower ductility, see Table 1. The intermediate areas present ferritic bainitic microstructures.

The SCC test method involves tapered tensile test specimens that are subjected to tensile stresses immersed in the appropriate electrochemical conditions. It is based on the method developed by the American Gas Association, Report 146 of Project NG-18 [10]. These tests allow the following data to be obtained for each material:

- threshold stress σ_{TH}: stress below which no cracks initiate, and
- crack propagation rate

Specimens were cut from base and weld materials of two tracts of pipe from different manufacturers, from now on referred to as Line 1 and Line 2. Fig. 1 shows weld and base metal specimens, respectively; the cutting process is also indicated. Two tests were carried out for each base material. Duration of tests was between 10 and 19 days.

Base metal samples were tapered. The applied load in tapered specimens was such that the maximum stress applied in the smallest section reached the yield stress of each material. As we move away from the smallest section, the stress decreases since the area increases, allowing in a single test to embrace a wide stress spectrum, which could later be correlated with operating pressures. SCC tests in

Table 1
Tensile and fracture toughness properties of base and seam weld metals of tested pipelines

Tube material	Yield strength Sy (MPa)		UTS (MPa)		Elongation (%)		Reduction of area (%)		Fracture toughness K_{IC} (MPa $m^{1/2}$)
	Long.	Circ.	L	C	L	C	L	C	C
Base	395	450	518	540	32	18	64	43	50
Weld	593	450	721	540	23	7	48	21	37

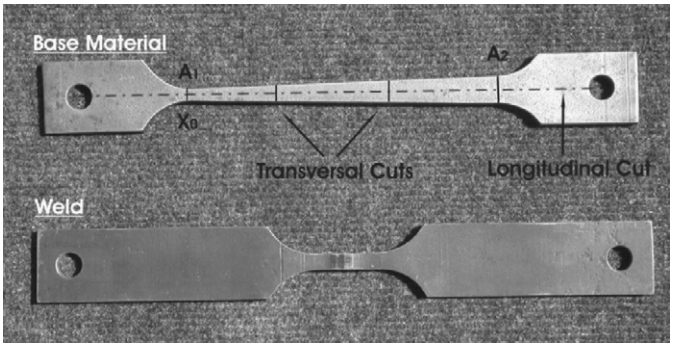

Fig. 1. Weld and base metal specimens. Cutting process is also indicated.

ERW metals require preserving natural crack initiation sites at the outer surface of the pipe. In order to faithfully reproduce metallurgical and surface conditions of the ERW, weld metal samples were cut transversely to the seam. Due to the small transverse dimension of the weld, these specimens were of constant section. The limitation imposed by the geometry of weld specimens made it necessary to conduct a series of tests at different load levels. Tests on these weld metal specimens were repeated under decreasing loads, until the applied stress under which cracks did not initiate was obtained.

The specimens were subjected to cyclic tensile stresses in a "walking beam" test machine that allows forces of up to 25,000 N to be applied through a lever arm. By means of an electric motor, a timer, a gear box and a cam, a helical spring is displaced once an hour, applying a variable load on the weights that reduce the applied load. The displacement is maintained during a period of half an hour, so that the applied stress on the specimen has a 1-h cycle (27×10^{-5} Hz).

The chemical composition of the solution in the electrochemical cell surrounding the specimen is: 53 g of Na_2CO_3 and 84 g of $NaHCO_3$ per liter of distilled water. The pH measured at room temperature was from 10.9 (previous to the tests) to 9.9 (after the tests). Potential was maintained constant at −750 mV with respect to saturated calomel (SCE), range reported as giving the highest susceptibility to SCC [12]. Stability of the reference electrode was checked before and after each test. The SCE reference electrode was maintained below 60 °C, communicated to the cell by a Lugging capillary. The experimental set-up is completed with an electrochemical cell made of carbon steel that acts as a counter electrode.

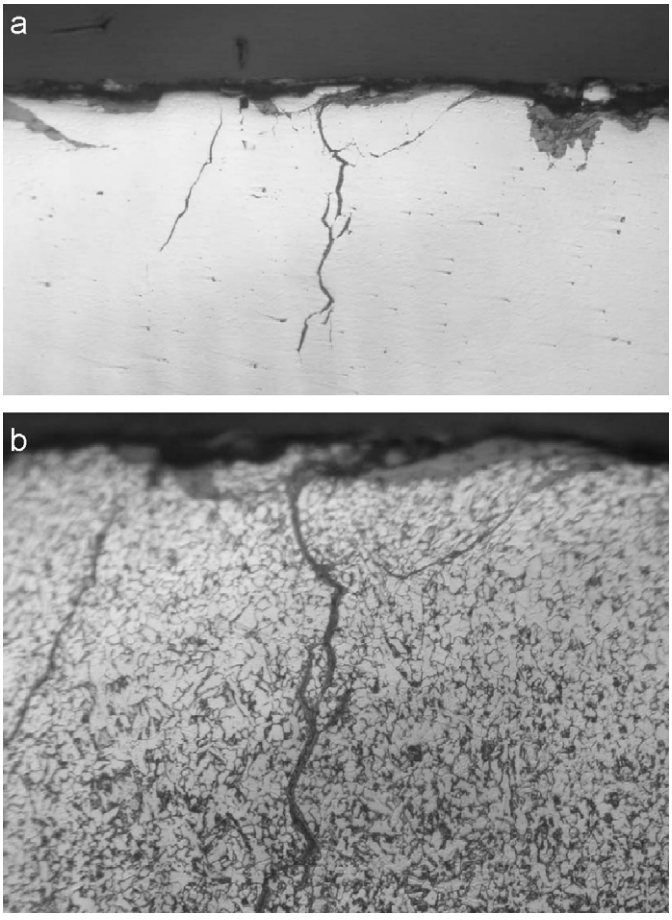

Fig. 2. (a) SCC crack, × 100. (b) SCC crack after Nital etching, × 200.

It is generally acknowledged that higher temperatures lead to higher SCC susceptibility, laboratory tests demonstrated that the steels used in pipelines can be susceptible to SCC up to temperatures of 90 °C [10]. The temperature of the first test was set at 73 °C (tolerance 2 °C), to accelerate the test while preventing evaporation and decomposition of the solution. Heating was provided by electric resistance.

After each test, the specimens end up covered with a black magnetite film. Metallographic specimens were prepared from sections longitudinal to the specimens. The length of each crack and its position relative to the smallest section of the tapered specimen was defined by optical microscopy. All cracks longer than 10 μm were detected and measured. As an example, Fig. 2 ((a) × 100, (b) × 200) shows one such crack in ERW metal of line 2, before and after Nital etching.

The experimental data for each material, along with fractographic, microstructural and fracture mechanics characterizations, make it possible to define the susceptibility to SCC of each material. The applied stress σ_x is related to the distance to the smallest section (X) in the tapered specimen:

$$\sigma_x = P/[A1 + ((A2 - A1)/L)X], \quad (1)$$

where P is the applied load, $A1$ the minimum section of the specimen, $A2$ the maximum section of the specimen and L the specimen length.

The threshold stress σ_{TH} is defined by the position of the smallest section in which no cracks were detected, $X_{TH.}$, and is related to the working pressure in the pipeline to define the threshold pressure P_{TH}, that is, the operating pressure below which SCC should not be expected:

$$P_{TH} = 2\sigma_{TH}t/D, \quad (2)$$

where t is the nominal thickness of the pipeline (6.35 mm), and D the outer diameter of the pipeline (350 mm).

To define the crack propagation rates, it is necessary to differentiate the two crack development stages: initiation and propagation. According to the results of previous studies on similar materials reported by AGA, a period of initiation of 3 days was estimated. Although the number of specimens in this study is too small to be statistically valid, regression of crack depths in base metal with time seems to agree with the 3-day time for crack initiation.

As an example, Fig. 3a and b plots the average length of the three longest cracks per mm of sample, as a function of X, for two tests in base metal of Line 1. X_{TH} is 46 mm, so that $\sigma_{TH} = 205$ MPa. The average crack propagation rate is 2.13 μm/day, or 7.7×10^{-4} m/year. Fig. 4 shows results for base metal of Line 2. In this case $X_{TH} = 15$ mm, $\sigma_{TH} = 278$ MPa. The average crack propagation rate is 2.3 μm/day, or 8.4×10^{-4} m/year. Note that the threshold stress for base metal of Line 1 is much smaller than for Line 2.

Estimated propagation rates at 75 °C were high, especially for the welds. Therefore, predicted lives are expected to be unrealistically short. On the one hand, the real effect of temperature on SCC cracking in ERW of Lines 1 and 2 is unknown. On the other hand, estimations of growth rates are strongly influenced by the estimates of the nucleation times, based on literature data for base metal. Therefore, new tests were carried out in ERW metal of Lines 1 and 2 to determine initiation times and growth rates at 45 °C. Applied loads were selected in such a way as

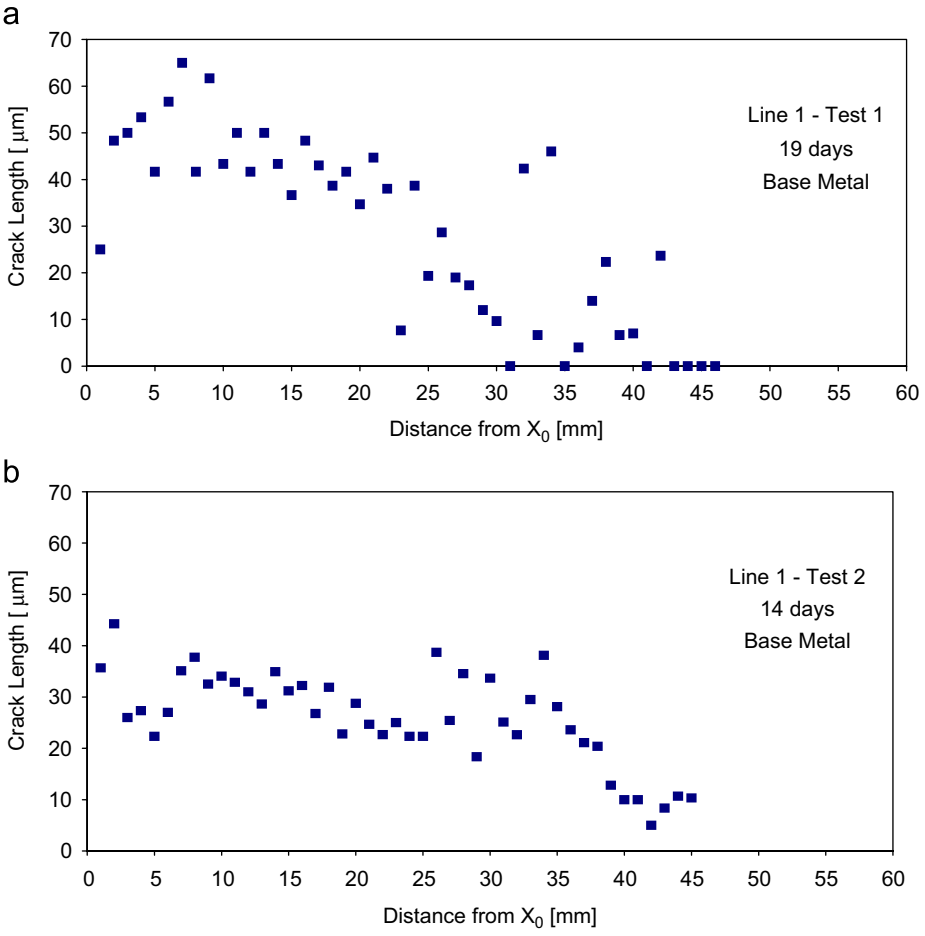

Fig. 3. (a) Average length of the three longest cracks per mm of sample, as a function of X. Base metal Line 1, Test 1. (b) Average length of the three longest cracks per mm of sample, as a function of X. Base metal Line 1, Test 2.

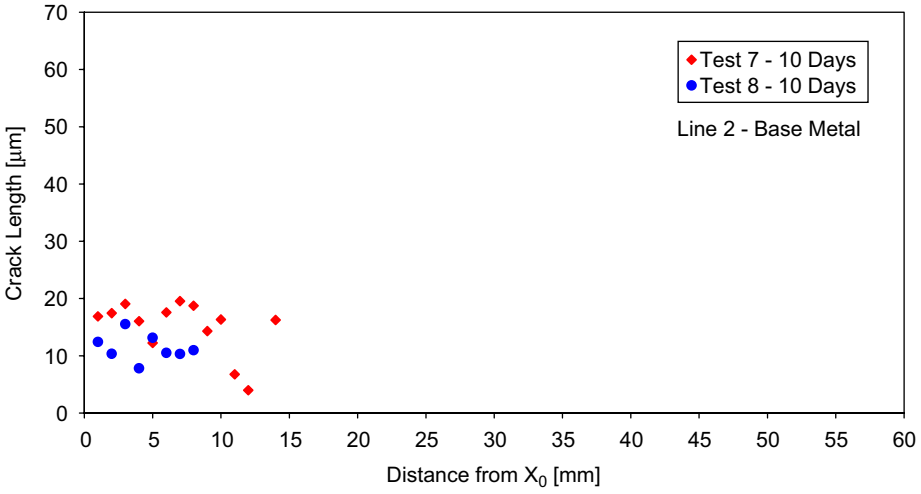

Fig. 4. Average length of the three longest cracks per mm of sample, as a function of X. Base metal Line 2, Tests 1 and 2.

Table 2
SCC test data for ERW materials of two API X42 pipelines: L1 and L2

Sample no.	Stress (MPa)	Equivalent pressure (MPa)	Cracked?	Test time (days)	Temp. (°C)	Max. crack length (µm)	Estimated max. growth rate	
							µm/day	mm/year
L1–3	372.99	13.32	Yes	11	73	110	13.8	5.0
L1–4	165.94	5.92	Yes	11	73	145	18.1	6.6
L1–5	124.22	4.43	Yes	11	73	50	6.3	2.3
L1–6	82.81	2.95	Yes	14	73	26	2.4	0.9
L1–9	103.60	3.70	Yes	11	73	83	10.4	3.8
L1–12	93.21	3.32	No	12	73	0	0.0	0.0
L2–10	142.32	5.08	Yes	10	73	320	45.7	16.7
L2–11	118.22	4.22	Yes	10	73	220	31.4	11.5
L2–13	130	4.64	Yes	11	73	580	72.5	26.5
L1–15	224.00	8.00	No	46	45	0	0.0	0.0
L1–17	223.85	7.99	No	79	45	0	0.0	0.0
L2–14	226.56	8.09	Yes	30	45	290	10.7	3.9
L2–16	223.93	7.99	Yes	30	45	263	9.7	3.6

to simulate an operating pressure of 8 MPa, and cycled as already described for 1 h periods.

3. Experimental results

Table 2 shows test data for all SCC tests on weld metal of Lines 1 and 2. The first two sets correspond to weld metal of both lines, tested at 73 °C. Due to the initial misinterpretation of data, tests on Line 2 did not reach the threshold stress, while the threshold stress for Line 1 can be estimated as between the stresses for samples 9 and 12.

Note also that estimated crack growth rates are much larger for weld material of Line 2. Trends are inverted when considering the last two sets, corresponding to tests at 45 °C (operating temperature). Although test times were longer, no cracks were found in tests on Line 1 weld metal, while cracks developed on Line 2 in the same conditions, although with much lower estimated growth rates than at 73 °C. There is some apparent inconsistency in the results of samples 6 and 12, the one with a slightly higher stress did not show cracks, meaning it was tested below the threshold stress, while some small cracks were found in the other, tested at a slightly lower stress. Since crack initiation is strongly dependent on surface conditions, this behavior is believed to be related to the particular conditions of the weld surfaces in each sample.

Literature data [13] for similar steels indicate that a decrease in temperature from 73 to 45 °C decreases propagation rates by a factor of 3.5. The maximum temperature of the pipeline is around 45 °C, so that a factor of 3.5 could relate the experimental SCC rates at 73 °C and SCC behavior under worst operation conditions (immediately downstream from pumping stations). These growth rates are shown in Table 3, along with the experimental data.

Table 3
Estimates of threshold stress and average propagation rates from experimental data and literature correlations, for base and ERW materials of L1 and L2 pipelines

Material	Threshold stress (MPa) 73 °C	Average crack growth rate (mm/year)			Threshold pressure (MPa)
		73 °C	45 °C estimate	45 °C experim.	
Base Line 1	258	0.77	0.256	–	8.0
Base Line 2	344	0.84	0.279	–	10.8
ERW Line 1	93–103	3.72	1.216	–	2.4
ERW Line 2	<118	18.23	5.20	3.75	<2.9

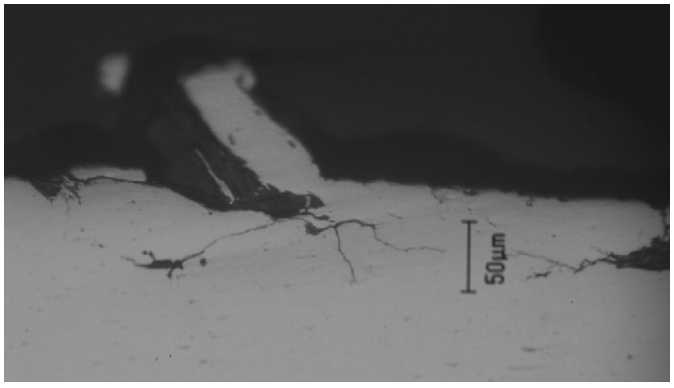

Fig. 5. Cracks in ERW Line 1, Test 3.

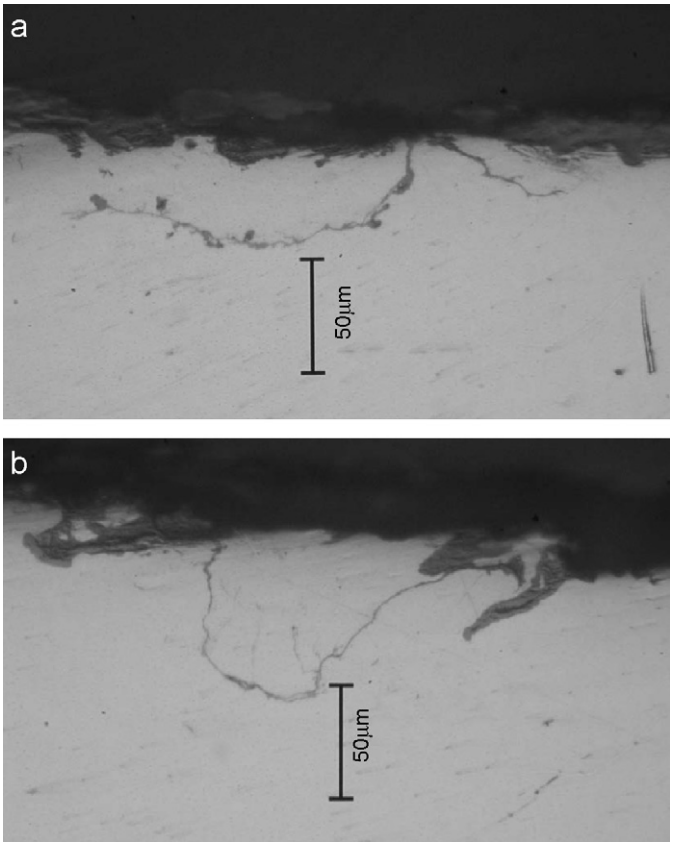

Fig. 6. (a) Cracks in ERW Line 1, Test 4. (b) Cracks in ERW Line 1, Test 4.

Cracks between 10 and 580 µm depth were found. Several interesting results can be drawn from the micrographic analysis of these cracks. Some cracks have a very different aspect ratio from those found in base metal tests and in SCC failed pipes, especially those that are very short, see for example Fig. 5. Note in this figure how chips or small pieces of metal were left on the pipe surface by the shaving process. Cracks initiated beneath these chips, which tend to be parallel to the surface rather than through the thickness. This was frequently found, and was related to the local through-thickness tensile residual stresses left by the shaving process. Once SCC cracks grow beyond this area, which is around 0.05 mm deep, they orient themselves through the thickness, as seen in Fig. 3.

Many of these small, arbitrarily oriented cracks become non-propagating when they reach a depth of 0.05 mm, see for example Figs. 6a and b. The combined effect of the surface defects and subsurface residual stress field results in a much lower number of relatively deep SCC cracks, when compared with SCC colonies in base metal, both in laboratory tests and in actual failure analyses [7]. Fewer cracks mean that load shedding effects, which tend to reduce crack driving forces in parallel cracks [14], are reduced. This is probably one of the reasons for the much larger SCC crack growth rates found in ERW metal when compared with those of base metal, as seen in Table 3. This can also be related to the unexpectedly high growth rate of only one crack in sample 13.

Sometimes it is difficult to differentiate whether initiation of these small cracks is truly due to SCC or may also be related to embrittlement due to plastic deformation. The true nature of all cracks identified as due to SCC was identified at higher magnifications, see for example Fig. 7a and b (× 500). These cracks show typical intergranular and branched propagation, indicative of SCC propagation.

Not all cracks were initiated at surface weld defects, see for example Fig. 8a, and yet some of these are still non-propagating when they reach a depth of less than 0.1 mm, see for example Fig. 8b. This is because there seems to be an additional effect of microstructure. As seen in Fig. 9b, the outer layer of the weld metal is mostly an equiaxial ferritic pearlitic microstructure, similar to that of a typical

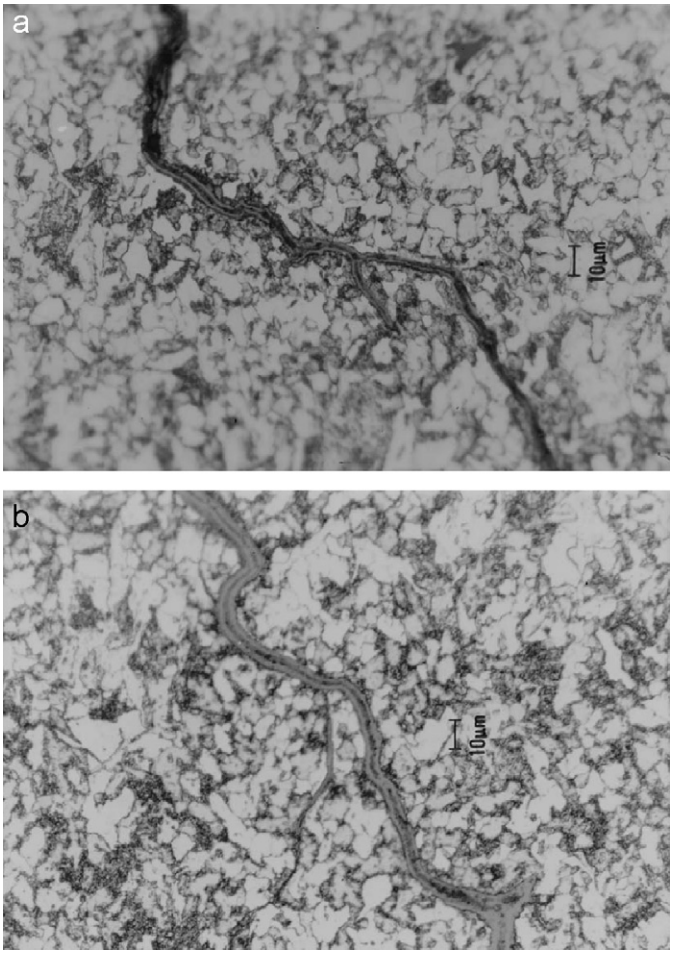

Fig. 7. (a) Cracks in ERW Line 2, Test 16. (b) Cracks in ERW Line 2, Test 13.

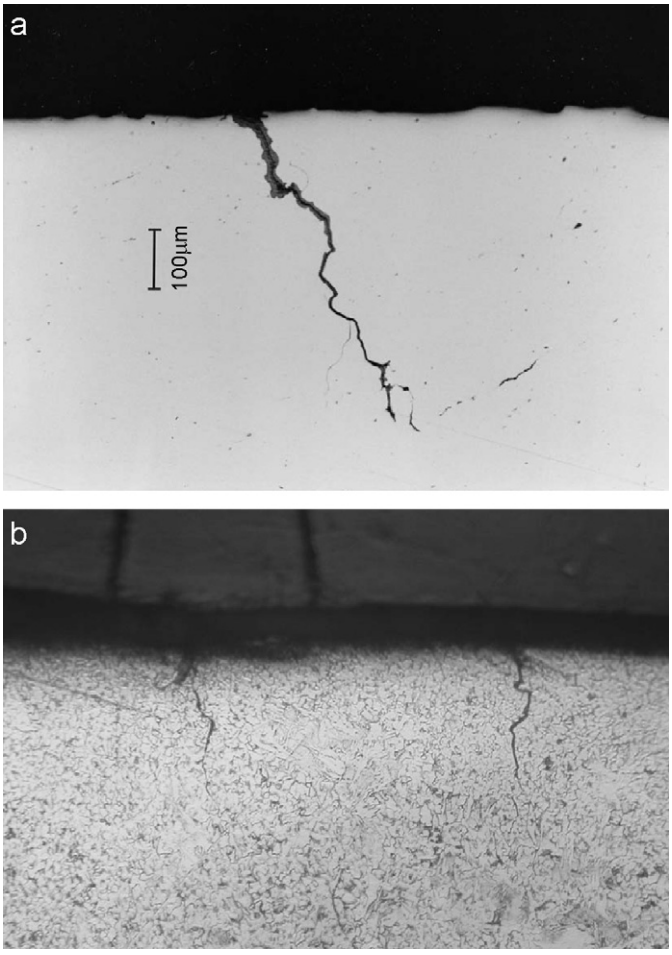

Fig. 8. (a) Longest crack found, 580 μm, in ERW Line 2, Test 13. (b) Cracks in ERW Line 2, Test 11.

base metal of an API 5L grade steel. This microstructure is well known for being susceptible to high pH SCC, as shown by the numerous in-service failures. Most of the section of the ERW weld is, on the other hand, composed of laminar microstructures, typical of the high deformation and cooling rates found in the mid-section of the welds. This microstructure is seen in the lower part of Figs. 8a and b, and in more detail in Fig. 9 (× 200). These bainitic or martensitic microstructures concentrate in a thin layer at the mid-plane of the ERW weld. This may be the reason why all cracks in ERW metal have been found to initiate at regions close to this mid-plane but never at it. On the other hand, these microstructures are brittle, so new welding procedures are designed to avoid them.

There are two sources of experimental error: the one due to estimating nucleation time has already been discussed. The other one is related to how much of the crack growth can be related to the experimental conditions, and how much could be the result of previous damage, such as fabrication cracks and SCC propagation during the 45-year previous service of the tested pipes. Note that these two possible errors go in opposite directions, the first tends to underestimate growth rates and the second tends to overestimate them. The micrographic study gave some evidence that weld defects were probably not larger than 50 μm, so that this value would not greatly influence the larger values of growth rates, based on cracks as large as 500 μm. Previous in-service SCC cracks can be ruled out,

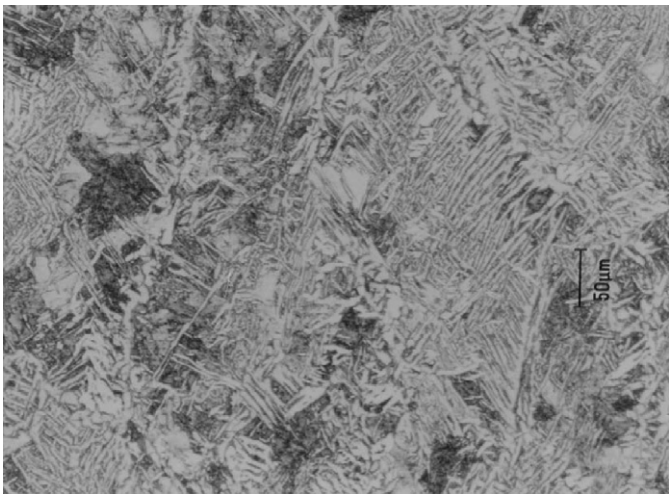

Fig. 9. Microstructure of ERW Line 2, sample 14 (× 200).

Table 4
SCC crack growth rates in laboratory tests

Source of data	Condition	SCC crack growth rates	
		mm/s	mm/year
Parkins et al. [15]	75 °C, −0.65 V	3.7×10^{-8}–8.3×10^{-8}	1.0–2.6
Beavers et al. [16]	75 °C, −0.65 V	10×10^{-8}–50×10^{-8}	3.15–15.7
Base metal	75 °C, –0.75 V	2.4×10^{-8}–2.7×10^{-8}	0.77–0.84
Weld metal	75 °C, –0.75 V	11.7×10^{-8}–57×10^{-8}	3.72–18.23

since the specimens were taken from sections without signs of coat disbonding or carbonate deposits.

Experimental growth rates for base and weld metals at 75 °C are compared in Table 4 with data from other sources for base metal in a similar steel pipe. It is concluded that the present growth rates are compatible with those found in the literature. Present data for base metal lie in the lower part of the range, while weld metal data lie in the upper part.

Crack growth rate estimates at 45 °C (Table 3) average 0.27 mm/year for base metal, and 3.2 mm/year for weld metal.

Weld metal SCC growth rates are around an order of magnitude larger than those for base metal. Base metal values compare very well with ranges found by other authors, based on base material data for in-service buried pipelines:

- Leis [17] reports average in-service crack growth rates in pipes that failed by an SCC of 1.6×10^{-8} mm/s (0.504 mm/year).
- Urednicek et al. [18] reports average growth rates of 8.5×10^{-9} mm/s (0.268 mm/year) in buried pipelines with 12–17 years in service.
- CEPA [19] publishes growth rates of 1×10^{-8} and 2×10^{-8} mm/s (0.31 and 0.63 mm/year) for NPS 36 and rates of 5×10^{-9} mm/s (0.157 mm/year) for NPS 8 and NPS 10, whereas cracks adjacent to the one that failed had growth rates of 1.4×10^{-9} mm/s (0.044 mm/year).

4. Consideration for life estimates under operating conditions

4.1. Tracts of the pipeline susceptible to SCC

The first step in evaluating the integrity of pipelines to SCC is to determine the tracts of pipe potentially susceptible to this degradation mechanism. To define SCC threshold pressures, circumferential residual stresses must be added to the stresses due to internal pressure, to define the total service applied stresses in the pipe surface. To experimentally quantify these manufacturing residual stresses, a ring of tube was instrumented with strain gauges, see Fig. 10, and a longitudinal cut was made at the weld centerline. Deformations were measured during cutting;

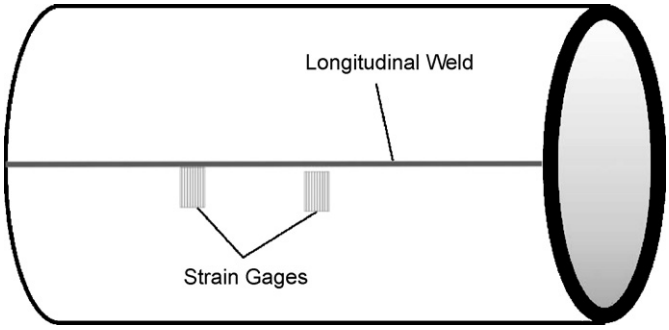

Fig. 10. Outline of residual stress measurement technique.

displacements were also recorded once the cut was finished. Measured deformations in the outer surface were translated into stress, and resulted in residual stress values of between 36.58 and 37.87 MPa. The displacement between cut edges was $Dx = 11$ mm, which was translated into stress using the simple mechanical model shown in Fig. 11. For this quarter of a ring subjected to a force H and a moment M, the solution is [20]

$$Dx/4 = [(\tfrac{3}{4}\pi - 2)HR^3 + (\pi/2 - 1)MR^2]/EI \quad (3)$$

with a radius R, a thickness t and a ring length L, giving a moment of inertia of the section I. For a $11/4 = 2.75$ mm displacement:

$$H = \sigma_m t L, \quad (4)$$

$$M = Lt^2\sigma_b/6, \quad (5)$$

$$\sigma_m + \sigma_b = 37\,\text{MPa}. \quad (6)$$

Substituting Eqs. (4)–(6) in Eq. (3), and iterating to get convergence:

$\sigma_m = 2$ MPa,

$\sigma_b = 35$ MPa.

This result is coincident with literature data: manufacturing residual stresses are for the most part self-balanced in the section (bending). So the maximun hoop residual stress in the pipe is 37 MPa, 10% of the yield stress and 16% of the service stress, considering the maximum operating pressure downstream from a pumping station. The residual stress is equivalent to an additional pressure Peq such that

$37\,\text{MPa} = P \times D/2t$

so that

Peq = 1.28 MPa.

Threshold pressure estimates for SCC initiation are summarized in the last column of Table 3, in which the equivalent pressure due to residual stress was subtracted. Since the threshold stress for the weld of Line 2 is not clearly defined, for practical purposes it could be conservatively considered identical to that of Line 1. SCC threshold pressures for these lines are controlled by the ERW welds. Therefore, in both lines the pipe tracts that are

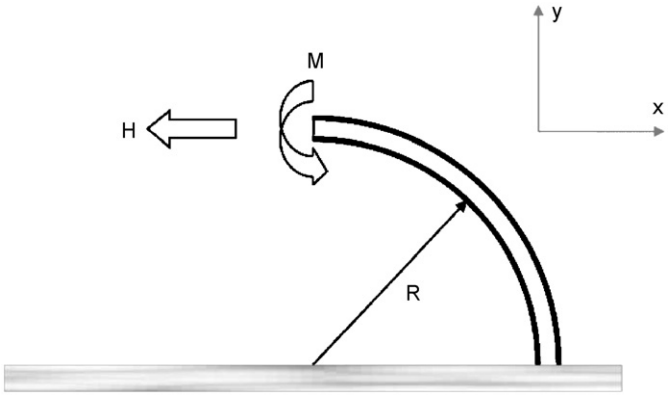

Fig. 11. Mechanical model used to translate displacement into stress.

considered to be susceptible to SCC are those that undergo a service pressure of at least 2.4 MPa. For the case under study, this represents about 70% of the pipe length. Only 30% of the pipeline, upstream of pumping stations, can be considered not susceptible to SCC.

4.2. Estimation of SCC lifetime

The catastrophic failure (blowout) of a pipeline takes place when one or more cracks grow beyond their critical size. Experimental results demonstrate that geometric discontinuities and small surface defects lead to the very early appearance of multiple cracks in the life of the component. These small cracks grow and coalesce to form a dominant crack. Knowing critical defect sizes and SCC propagation rates, an estimate of the time required for a crack of a certain depth to become critical could be easily carried out, using a fracture mechanics approach and the fracture toughness of base and weld materials (Table 1).

Table 5 shows the results of the remaining life estimation performed according to the procedures given in API RP 579 Section 9 [21]. The maximum crack depth that could survive a hydrostatic test at a pressure of 1.1 specified minimum yield strength (SMYS) is the critical crack depth at such pressure. This is the largest hypothetical crack that would remain in the pipeline after the test. The time for this crack to reach the critical depth at operating pressure (72% of SMYS) can be estimated as the ratio between the difference in critical crack depths Δa and the crack growth rate. Table 5 shows the results, considering an average crack growth rate at 45 °C for base metal (Table 3) and the lowest growth rate estimates for weld metal.

From the results shown in Table 5, it is seen that, due to the unexpectedly high SCC crack growth rates found in weld metal (around 3.2 mm/year), estimated remnant lives are very short. This analysis would yield periods for in-service inspection which are around 1 year, far less than the usual 5-year periods accepted now in the industry. A prediction such as this makes an approach based on periodic non-destructive evaluations (ILI) or hydrostatic re-tests of the pipeline impractical.

Table 5
SCC life-time estimation from previous hydrostatic test

	Critical crack depth a_c (mm)	Δa (mm)	Growth rate (mm/year)	Remaining life (years)
Base material				
1.1 SMYS	4.5	1.4	0.27	5.2
0.72 SMYS	3.1			
Weld				
1.1 SMYS	3.5	1.2	1.2	1
0.72 SMYS	2.3			

A key factor is to find out for how much of the service time the actual conditions in the pipe surface are sufficient for SCC crack growth to occur. Of the three main factors controlling SCC in buried pipelines, pressure, CP potential and temperature are approximately constant during the year. The degree of humidity is the main controlling factor: it is known that SCC failures tend to occur in regions with periodic floods followed by dry soil conditions. These intermittent conditions mean that the average in-service SCC growth rate in buried pipelines will be a fraction of the experimental growth rates. The definition of a 5-year service period between hydrostatic tests, which is used nowadays and based on empirical field data, would indicate that the conditions for SCC crack growth are found in less than 20% of the year. These tests are nowadays carried out at 110% of SMYS of pipe base metal, and are one of the best ways of mitigating SCC damage. Under these conditions, all the service cracks that are near the critical condition (close to cause blow out) would fail during the test, and those that do not fail are sure to require a long enough time to grow before becoming critical. Compressive residual stresses at crack tips further reduce growth rates.

The aforementioned aspects allow us to conclude that an inspection strategy based on crack growth rates is at this time not yet recommended. Rather than that, a strategy based on identifying the susceptible regions of the pipelines seems better adapted for a strategy to deal with the integrity of pipelines subjected to high pH SCC. In order to improve the usefulness of such an approach, a clear understanding of the conditions that could lead a propagating SCC colony to finally produce a blow-out or only a leak would be of value. One way is to analyze the interaction conditions of multiple growing cracks. How interaction affects growth rates may not be the most important aspect. How this interaction influences the stress states and crack driving forces at different points of the crack fronts, which are controlled by load shedding and plasticity of the ligaments between neighboring cracks, affects both the possible arrest of cracks and the leak before break condition at the moment of final rupture. All these factors are mostly related to the SCC threshold pressure, which is a more reliable experimental value and less affected by service conditions than growth rates.

5. Conclusions

Threshold stresses and crack growth rates for in-service SCC cracking of two ERW seam welded oil pipelines were experimentally assessed. Seventeen high pH SCC tests were carried out in specimens taken from two 45-year-old oil pipelines, in both base and ERW weld metals, at two temperatures (73 and 45 °C). Tapered specimens were used for base metal; constant section specimens were developed for ERW tests, in which original surface conditions were preserved.

SCC threshold stresses and crack growth rates for base material did not present difficulties, initiation times in base metal seem to be around 3 days, matching values proposed in the literature.

It was found that SCC crack initiation at welds is strongly influenced by local geometry, weld defects and localized through-thickness residual stresses due to the shaving process during pipe manufacturing. Previous defects are responsible for the nucleation of smaller cracks, which lead to higher crack growth rates and lower threshold stresses. All these result in much higher susceptibility of the ERW seam welds than those for base materials, so that the welds define the length of the pipeline that is susceptible to SCC.

Circumferential residual stresses were experimentally measured, in order to have a better estimate of SCC threshold pressures. Maximum residual stresses were around 37 MPa, at the outer surface of the pipes.

SCC threshold pressures for these lines are controlled by the ERW welds, the pipe tracts that are considered to be susceptible to SCC are those that undergo a service pressure of at least 2.4 MPa. For the cases under study, this represents about 70% of the length of the pipeline.

Acknowledgments

This research work was funded by Grant PIP 6257 from CONICET (Consejo Nacional de Investigaciones Científicas y Técnicas de la República Argentina), CIC (Comision de Investigaciones Científicas de la Provincia, Buenos Aires, Argentina) and Grant PICTO 12-609/04 by Agencia Nacional de Promocion Cientifica, Argentina.

References

[1] McCLure GM. Field failure investigations. Symposium on pipe line research. Dallas, TX, USA, 1965.
[2] Jones DJ. An analysis of reportable incidents for natural gas transmission and gathering lines 1970 through June 1984. NG 18 Report No 188. American Gas Association, Catalog no. L51499, 1986.
[3] Hussain K, Shaukat A, Hassan F. Corrosion cracking of gas-carryinng pipelines. Mater Perform 1989:13.
[4] Wenk RL. Field investigation of stress corrosion cracking. American Gas Association, Catalog no. L30174, 1974. p. T-1.
[5] Parkins RN, O'Dell CS, Fessler RR. Factors affecting the potential of galvanostatically polarised pipeline steel in relation to SCC in co2–3-hco-3 solutions. Corros Sci 1984;24:343–73.
[6] Fessler RR. Stress corrosion cracking temperature effects. V Symposium on line pipe Research, Houston, TX, USA, 1979.
[7] Manfredi C, Otegui JL. Failures by SCC in buried pipelines. Eng Failure Anal 2002;9:495–509.
[8] Otegui JL, Chapetti MD, Motylicki J. Fatigue assessment of an ERW oil pipeline. Int J Fatigue 2002;24:21–8.
[9] Kiefner F, et al. Failure analysis of pipelines. ASM Handbook, ASM International; 1997.
[10] NG-18 Report 146. Test method for defining susceptibility of pipe line steels to stress-corrosion-cracking. American Gas Associatión, 1985.
[11] API 5L Specifications for Line Pipe. 41st. ed. American Petroleum Institute; 1995.
[12] Parkins RN, et al. Stress corrosion cracking characteristics of a range of pipeline steels in carbonate-bicarbonate solution. Corrosion 1993;46:951.
[13] Berry WE. Sress corrosion cracking laboratory experiments. V Symposium on line pipe research. AGA, paper V, Dallas, 1974.
[14] Wessel C, Cisilino A, Santi O, Otegui J, Chapetti M. Numerical and experimental determination of three dimensional multiple crack growth in fatigue. Theor Appl Fract Mech 2001;35:47–58.
[15] Parkins RN, Belhimer E, Blanchard WK. Stress corrosion cracking characteristics of a range of pipeline steels in carbonate bicarbonate solutions. Corrosion 1993;49(12):951.
[16] Beavers JA, Berry WE, Parkins RN. Mater Perform 1986;25(6):9.
[17] Leis BN. Average cracking speed as a function of operating conditions for stress corrosion cracking in pipelines—site specific, climatic and stress history effects. EPRG/PRC 10th Biennial Joint Technical Meeting on Line Pipe Research, Cambridge, UK, April 1995.
[18] Urednicek M, Lambert S, Vosikovski S. Stress corrosion cracking monitoring and control. Paper 7-2 Conference on Pipeline Reliability, 1992.
[19] Canadian Energy Pipeline Association. Stress corrosion cracking, recommended practices, 1997. p. 71.
[20] Roark RJ. Formulas for stress and strain. 4th ed. New York: McGraw-Hill; 1965.
[21] API Recommended Practice 579: fitness for service. 1st ed. American Petroleum Institute; January 2000.